Magnetic phase diagram of antiferroquadrupole ordering in HoB_2C_2

Tatsuya Yanagisawa,* Terutaka Goto, and Yuichi Nemoto
Graduate School of Science and Technology, Niigata University, Niigata 950-2181, Japan

Ryuta Watanuki
Institute for Solid State Physics, University of Tokyo, Kashiwa, Chiba 277-8581, Japan

Kazuya Suzuki
Graduate School of Engineering, Yokohama National University, Yokohama 240-8501, Japan

Osamu Suzuki and Giyuu Kido
National Institute for Materials Science, Sakura, Tsukuba 305-0003, Japan
(Received 14 October 2004; revised manuscript received 4 January 2005; published 24 March 2005)

The magnetic phase diagram for antiferroquadrupole (AFQ) ordering in tetragonal HoB_2C_2 has been investigated by measurements of elastic constants C_{11}, C_{44}, and C_{66} in fields along the basal x-y plane as well as the principal [001]-axis. The hybrid magnet (GAMA) in Tsukuba Magnetic Laboratory was employed for high field measurements up to 30 T. The AFQ phase is no longer observed above 26.3 T along the principal [001]-axis in contrast to the relatively small critical field of 3.9 T in fields applied along the basal [110]-axis. The quadrupolar intersite interaction of O_{xy} and/or O_2^2 is consistent with the anisotropy in the magnetic phase diagram of the AFQ phase in HoB_2C_2.

DOI: 10.1103/PhysRevB.71.104416 PACS number(s): 74.25.Ld, 71.55.Ak, 62.65.+k

I. INTRODUCTION

$4f$-electron systems, with orbital as well as spin degrees of freedom, in rare earth compounds frequently show electric quadrupole ordering in addition to magnetic dipole ordering at low temperatures. We noted that in HoB_6, with a Γ_5 triplet ground state, ferroquadrupole ordering is accompanied by a structural change from a cubic lattice to a trigonal one.[1–3] CeB_6, with a Γ_8 quartet ground state, is well known as a typical example of antiferroquadrupole (AFQ) ordering in a cubic compound.[4–6] The tetragonal lanthanide compounds DyB_2C_2, HoB_2C_2, and TbB_2C_2 are also known to show AFQ ordering in competition with antiferromagnetic (AFM) ordering.[7–9] These systems have the tetragonal LaB_2C_2-type structure[10–12] with space group $P4/mbm$ as shown in Fig. 1(a). The specific heat and magnetic susceptibility measurements performed by Yamauchi *et al.* revealed that DyB_2C_2 exhibits quadrupole ordering of the Dy^{3+} ($J=15/2$) ions in phase II below $T_Q=24.7$ K, which successively transits to an AFM state in phase III at $T_N=15.3$ K.[7] Neutron diffraction measurements have shown the characteristic AFM structure, with a slightly tilted angle, lying in the tetragonal basal plane.[11,12] The tilting of magnetic moments in the phase III are attributed to the competitive intersite interactions between the AFM and AFQ moments. Furthermore, field induced AFM moments of the AFQ phase II in the basal plane were detected by neutron scattering under magnetic fields applied along the [100]-axis.[13] Recently, Tanaka *et al.* performed detailed resonance x-ray scattering measurement at two resonant energies of electric dipole ($E1$) transition and electric quadrupole ($E2$) transition at the Dy^{3+} L_{III} absorption edge.[14,15] The $(0\ 0\ l/2)$ reflections at $E2$ channels of scattering suggests the anisotropic charge distribution below T_Q is consistent with the AFQ ordering in the basal plane. It was also reported that an anisotropic charge distribution due to a small buckling lattice distortion of the B- and C-atoms contributes to the main peak of the resonant x-ray spectra of the $E1$ transition in DyB_2C_2.[16–20] These results suggest that the O_{xy}- and/or O_2^2-type quadrupole ordering possessing a

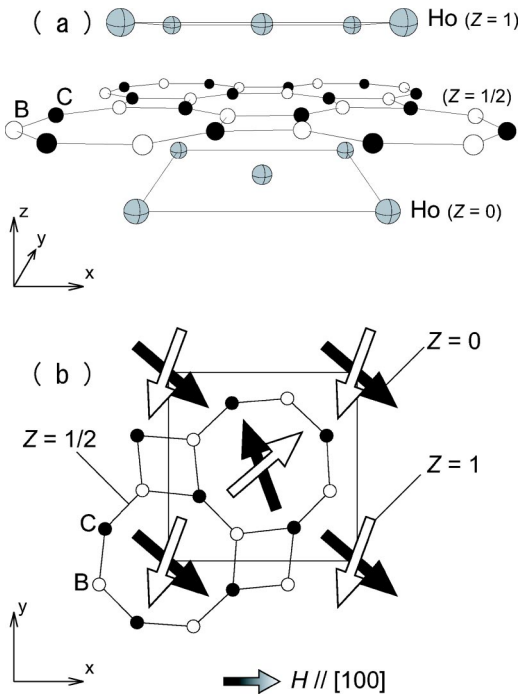

FIG. 1. The crystal structure of HoB_2C_2. (b) The magnetic structure applying $H\|[100]$ in phase III of HoB_2C_2, according to Ohoyama *et al.* (Ref. 21) and Zaharko *et al.* (Ref. 26).

TABLE I. Classification and summary of the phase on HoB_2C_2.

Phase	Properties	Reference
I	Paramagnetic, Paraquadrupole	8, 29
II	Antiferroquadrupole ordering (with field induced magnetic moments)	13–19,[a] 20, 27[b]
III	Antiferroquadrupole+Antiferromagnetic ordering (coexistence)	20 and 21, 26,[a] 27[b]
III′	Antiferroquadrupole+Antiferromagnetic ordering (with magnetic domains)	26[a]
III″	Antiferroquadrupole+Antiferromagnetic ordering (with partly reoriented magnetic moments)	7,[a] 25[a]
IV	Incommensurate magnetic ordering (with diffuse neutron scattering)	21, 22

[a]Results on DyB_2C_2.
[b]Results on $Ho_{1-x}Dy_xB_2C_2$.

charge distribution in the basal plane is the order parameter of phase II of DyB_2C_2.

Onodera *et al.* reported that an isomorphous compound HoB_2C_2 shows an incommensurate short range magnetic ordered phase IV at $T_{C1}=5.9$ K and successively undergoes an AFM ordering at $T_{C2}=5.0$ K in zero field.[8] The magnetic structure below T_{C2} on HoB_2C_2 is essentially the same as that of DyB_2C_2 [Fig. 1(b)]. The intermediate phase IV possesses a long periodic magnetic structure characterized by a propagation vector of $k=(1+\delta,\delta,\delta')$ with $\delta=0.11$ and $\delta'=0.04$, along with broad diffuse magnetic scattering around $k=(100)$.[21,22] The phase IV of HoB_2C_2 is contrast to the absence of that in DyB_2C_2. It is noted that neutron scattering on TbB_2C_2 and ErB_2C_2 also show long periodic magnetic ordering with nearly the same periodicity as HoB_2C_2.[23,24] We show, in Table I, a dyad of the phase classification and these properties on HoB_2C_2. Here, phase I is paramagnetic (paraquadrupole) phase. The phase III′ and III″ are subphase of phase III, which will be discussed later. Some references with superscripts indicate that the phase is identified by analogy from the results on DyB_2C_2 and $Ho_{1-x}Dy_xB_2C_2$.

Elastic constants representing quadrupole susceptibility of the $4f$-electron system is a useful probe for examining a ground state with orbital degeneracy or pseudodegeneracy in particular.[28] We have performed ultrasonic measurements on HoB_2C_2 and in Fig. 2 we present the measured elastic constants for comprehension.[29] Considerable softening of 22% for C_{44} below 100 K, 5.5% for C_{66} below 50 K, and 2.4% for $(C_{11}-C_{12})/2$ below 30 K down to $T_{C1}=5.0$ K indicate a pseudotriplet ground state consisting of E-doublet and A (or B) singlet in HoB_2C_2.[29] In phase IV, all transverse modes show enhanced softening associated with considerable ultrasonic attenuation, where slow relaxation time of $\tau\sim 7\times 10^{-9}$ s was found.

The magnetic field-temperature (H-T) phase diagrams of DyB_2C_2 and HoB_2C_2 show anisotropic behavior depending on the field directions.[8,25] The order parameter of the AFQ phase and its relation to the anisotropy of the H-T phase diagram still remain to be solved.[30] The H-T phase diagram of the AFQ phase II of tetragonal DyB_2C_2 and HoB_2C_2 compounds are often compared to that found in cubic CeB_6 (Refs. 4–6) and La-diluted systems $Ce_xLa_{1-x}B_6$.[31–33] It has been reported that $Ce_xLa_{1-x}B_6$ ($x=0.75-0.60$) exhibits an ordered phase IV being close to the AFQ and AFM phases. A huge softening in a transverse elastic constant C_{44} and a trigonal lattice distortion in the phase IV of $Ce_xLa_{1-x}B_6$ indicates a spontaneous ferroquadrupole moment.[34] Kubo and Kuramoto have recently proposed a plausible model based on octupole ordering to explain the trigonal distortion in phase IV.[35] The order parameter of phase IV in the present compound HoB_2C_2 is not settled yet. The competition between AFQ and AFM ordering in the tetragonal HoB_2C_2 system is an important issue in the present work.

We have performed ultrasonic measurements on single crystals HoB_2C_2 under magnetic fields in order to investigate the anisotropic behavior of the AFQ phase II in the H-T phase diagram in fields along the three principal axes $H\|[110]$, $H\|[100]$, and $H\|[001]$. In Sec. II the experimental procedure is described. The experimental results of the elastic constants and the magnetic phase diagrams are presented in Sec. III. The concluding remarks are in Sec. IV.

II. EXPERIMENTAL DETAILS

HoB_2C_2 single crystals were grown with a tetra-arc furnace. Rectangular samples with dimension of $3\times3\times2$ mm^3 and $2\times2\times3$ mm^3 were prepared by a wire discharge cutter for the ultrasonic measurement. The orientation of crystal with respect to applied magnetic field was settled with in the accuracy of 1 degree by using x-ray Laue diffractions. The $LiNbO_3$ transducers for the generation and detection of the sound waves with the frequencies 8.5 MHz and its overtone 31 MHz were bonded on opposite surfaces of the sample. An ultrasonic apparatus based on the phase comparison method, detecting time-delay for successive ultrasonic echo signals, was used to measure the sound-velocity v. For the estimation of the elastic constant $C=\rho v^2$, we used the mass density $\rho=6.965$ g/cm^3 from the lattice parameter $a=b=0.534$ nm and $c=0.352$ nm of HoB_2C_2. A ^{3}He-evaporation refrigerator was used for the low-temperature measurements down to 0.5 K. Magnetic fields

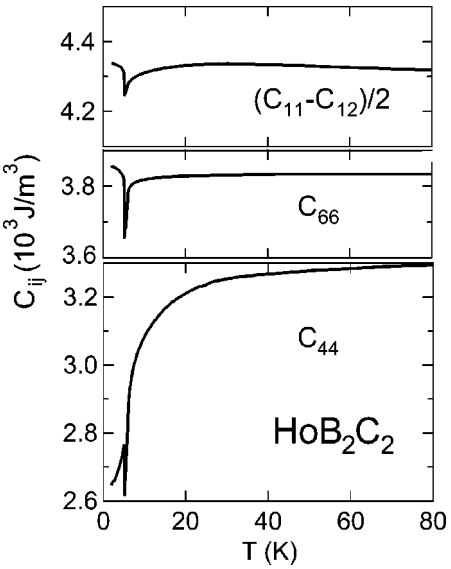

FIG. 2. Elastic constants of C_{44}, C_{66}, and $(C_{11}-C_{12})/2$ as a function of temperature below 80 K.

up to 12 T were applied by a superconducting magnet. Magnetic fields above 12 T were generated by a hybrid magnet (GAMA) consisting of the superconducting magnet and water-cooled resistive magnet in Tsukuba Magnet Laboratory (TML) of the National Institute for Materials Science (NIMS).

III. RESULTS AND DISCUSSION

A. Magnetic field dependence for $H\|[100]$ and $H\|[110]$

Figure 3 represents the relative change of elastic constant

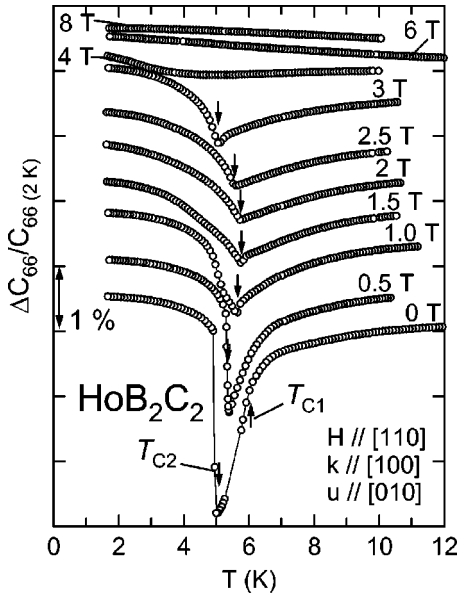

FIG. 3. Relative change of the elastic constant $\Delta C_{66}/C_{66}$ vs temperature under various magnetic fields applied along the [110]-axis of HoB_2C_2. Transverse modes at frequencies of 31 MHz were used for the measurements.

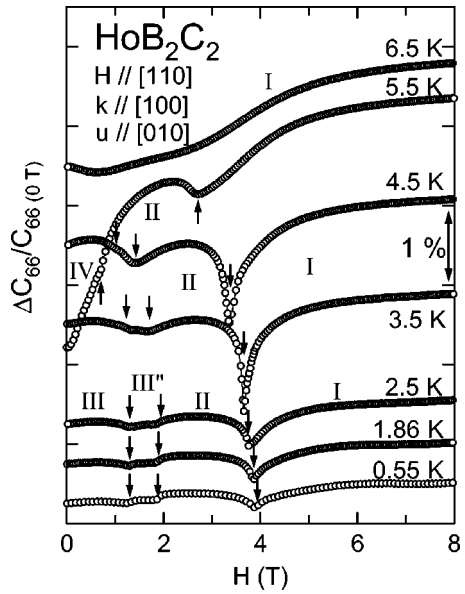

FIG. 4. Relative change of the elastic constant $\Delta C_{66}/C_{66}$ vs magnetic field at frequencies of 31 MHz under various temperatures in HoB_2C_2. Magnetic fields up to 8 T were applied along the [110]-axis.

C_{66} as a function of temperature under various magnetic fields for $H\|[110]$. The C_{66} was measured by the transverse ultrasonic mode propagating along the [100]-axis with polarization along the [010]-axis, corresponding to a symmetry strain ε_{xy} with a $B(\Gamma_2)$ representation. The transverse C_{66} exhibits a softening of 3% with decreasing temperature down to the transition temperature $T_{C2}=5.0$ K in zero field. The softening of C_{66} in the phase IV is suppressed in a magnetic field of 0.5 T, and T_{C1} of the I-IV transition point shifts to lower temperatures with increasing fields. The C_{66} increases below T_{C2} being the transition point from the phase IV to the phase III. Then these I-IV and III-IV transition points cross each other at a tetracritical point in *H-T* phase diagram [see Fig. 6(c)]. The minima of C_{66} in fields above 1.5 T and up to 3 T indicates transition from paramagnetic phase I to the AFQ phase II. Above 4 T, no indication of this phase transition was observed.

Figure 4 represents the relative change of the elastic constant C_{66} as a function of magnetic field for $H\|[110]$ at several temperatures. In temperatures below 4.5 K and down to 0.55 K, the sharp minima around 3.5–4 T suggest the occurrence of an I-II phase transition, which is expected in the ordered phase with symmetry breaking character. The intermediate region of two transitions, from 2 T to 4 T in $H\|[110]$, indicates the AFQ phase II. The small anomalies at fields lower than 1.9 T are an indication of the II-III phase transition. The III''_{110}-III phase transitions has been also observed at 1.7 T. A broad minimum at 6.5 K indicates no sign of the field induced phase transition.

The relative change of the elastic constant C_{44} as a function of magnetic field for $H\|[100]$ is shown in Fig. 5. The C_{44} was measured by a transverse ultrasonic mode propagating along the [100]-axis (or [010]-axis) with polarization along the [001]-axis. The C_{44} mode induces a symmetry

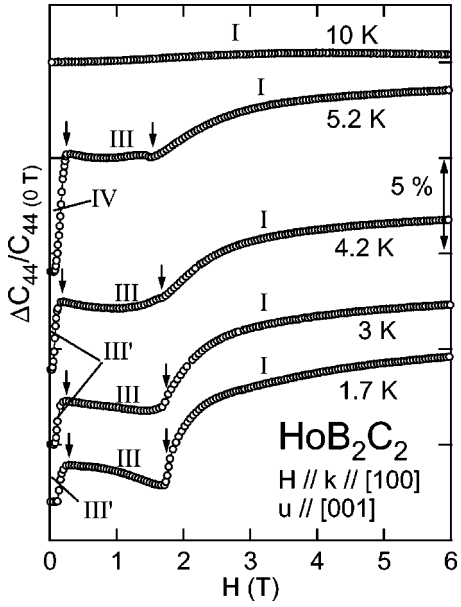

FIG. 5. Relative change of the elastic constant $\Delta C_{44}/C_{44}$ vs magnetic field at frequencies of 31 MHz under various temperatures in HoB_2C_2. Magnetic fields up to 8 T were applied along the [100]-axis.

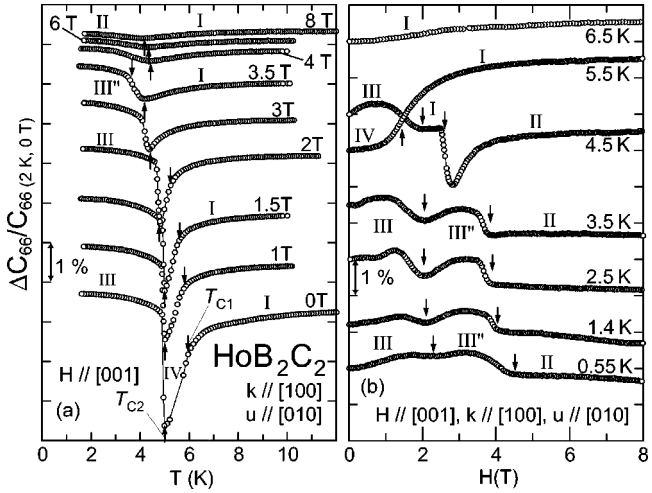

FIG. 7. Relative change of the elastic constant $\Delta C_{66}/C_{66}$ of the transverse modes at frequencies of 31 MHz under various fields and temperatures in HoB_2C_2. Fields up to 8 T were applied along the [001]-axis. (a) shows temperature dependence, (b) shows field dependence.

strain ε_{zx} (or ε_{yz}) corresponding to one component in $E(\Gamma_{34})$ doublet. The magnetic field dependence of C_{44} in Fig. 5 shows two anomalies, a kink at 1.8 T corresponding to the I-III phase transition and a step anomaly at 0.2 T. The latter transition shows hysteretic behavior, which may be caused by a domain effect in phase III.

In Fig. 6, we show the *H-T* phase diagram of HoB_2C_2 which was obtained by ultrasonic and magnetization measurements in fields applied parallel to the basal plane. Phase boundaries were determined by C_{66} vs H (solid triangles), C_{66} vs T (grey circles), C_{44} vs H (solid diamonds), and C_{44} vs T (solid reverse triangles). Open symbols show the results of magnetization measurements by Onodera *et al.*[8] In the phase diagram of Fig. 6(a) we use the previous ultrasonic results from Ref. 29. In order to verify the anisotropy of the AFQ phase II, the magnetic fields were applied along the intermediate direction with an angle $\theta=22.5°$ between the [100] and the [110]. Further details of the ultrasonic results are skipped in the present paper for convenience.

As one can see in Fig. 6, the AFQ phase II shows anisotropic behavior as a function of the field direction in the basal *x-y* plane. The upper critical magnetic field $H_{C[110]}=3.9$ T of the II-I transition for $H\|[110]$ shrinks to $H_{C[100]}=2.0$ T for $H\|[100]$, while the AFM phase III and the phase IV behave mostly in an isotropic manner being independent of the field direction in the basal plane. The order parameter of phase II has stability against field $H\|[110]$ more than $H\|[100]$. Actually, the phase II is stable only in the vicinity of the phase III-I boundary along $H\|[100]$ in Fig. 6(a).

B. Magnetic field dependence for $H\|[001]$

Figures 7(a) and 7(b) represent the temperature depen-

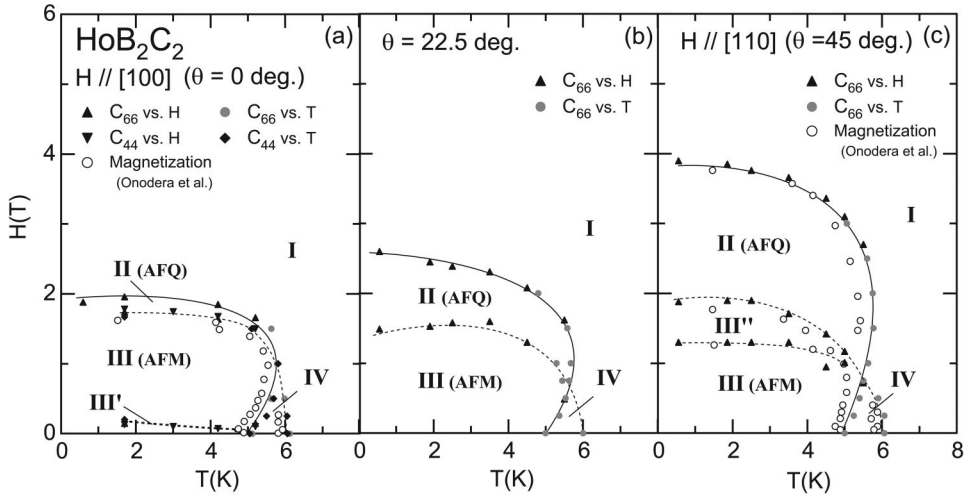

FIG. 6. *H-T* phase diagrams of HoB_2C_2 with the fields applied along the (a) [100], (b) $\theta=22.5°$, and (c) [110] directions. Data points were determined from the elastic anomalies in C_{66} vs H (solid triangles), C_{66} vs T (grey circles), C_{44} vs T (solid reverse triangles), and C_{44} vs H (solid diamonds) as shown in Figs. 3–5. Solid and dotted lines are guides for the eyes. Previous data of magnetization measured by Onodera *et al.* are also shown for comparison.

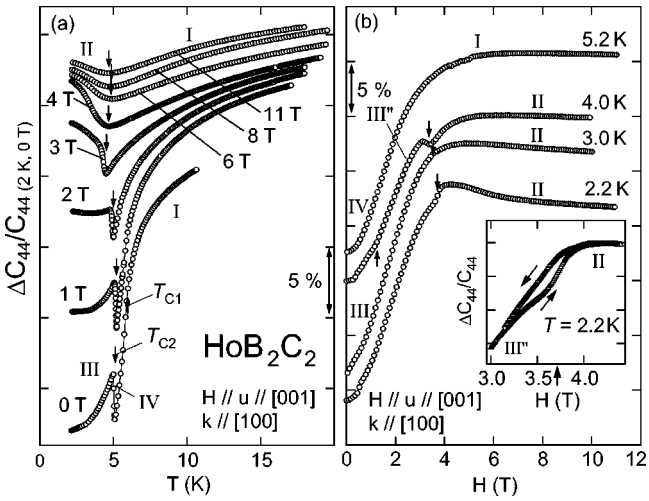

FIG. 8. Relative change of the elastic constant $\Delta C_{44}/C_{44}$ of the transverse modes at frequencies of 31 MHz under various fields and temperatures in HoB_2C_2. Fields up to 11 T were applied along the [001]-axis. (a) shows temperature dependence, (b) shows magnetic field dependence. Inset of (b) shows hysteretic behavior around 3.5 K.

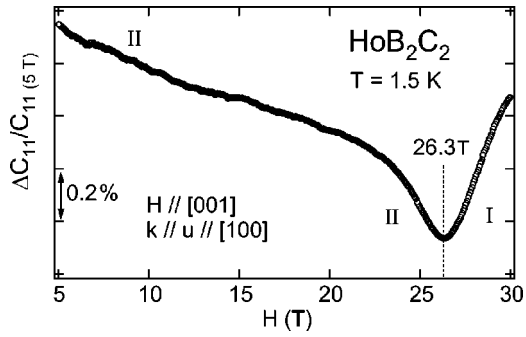

FIG. 9. Relative change of the elastic constant $\Delta C_{11}/C_{11}$ at a fixed temperature of 1.5 K displayed as a function of magnetic field along the [001]-axis up to 30 T. Measurement frequencies are 52 MHz.

dence of $\Delta C_{66}/C_{66}$ under various fields up to 8 T along the principal [001]-axis and field dependence at various temperatures, respectively. In Fig. 7(a), the I-IV transitions at T_{C1}=5.9 K, indicated by down arrows, shift to lower temperatures with increasing field up to 3 T while the IV-III transition T_{C2}, indicated by upward arrows, shift slightly to lower temperatures in field. Eventually T_{C1} and T_{C2} cross each other at 3 T. At 3.5 T, two anomalies indicating the successive transitions I-II and II-III were observed. The I-II transition has been found from 4 T to 8 T in Fig. 7(a). These transition points are shown in the phase diagram in Fig. 11. We successfully observed the AFQ phase II in high magnetic field applied along $H\|[001]$ above 4 T.

Magnetic field dependence of $\Delta C_{66}/C_{66}$ at temperatures from 0.55 K to 6.5 K is shown in Fig. 7(b). Two successive transitions of III-III$''_{001}$ and III$''_{001}$-II, indicated by arrows, are a common feature in the measurements performed at 0.55, 1.4, 2.5, and 3.5 K. At 4.5 K, a reentrant process of III-I-II phase transition was observed between 2 T to 2.7 T. At 5.5 K, the I-IV phase boundary shows a broad plateau around 1.4 T. At 6.5 K, C_{66} shows a monotonous increase in phase I. It should be noted that the tetracritical point exists at $T^* \sim 4.5$ K and in a field $H^* \sim 3$ T applied along the principal [001] direction. This point is argued again in the magnetic phase diagram of Fig. 11.

As shown in Fig. 2, the transverse C_{44} mode in zero field shows considerable softening on the order of 20% with decreasing temperature. The softening of C_{44} is very much reduced in applied fields along the principal [001] direction, as shown in Fig. 8(a). The sharp minima of C_{44} in fields below 3 T, shown by downward arrows, indicate the IV-III transition points. The I-IV transition points, which have clearly been observed in the results of C_{66}, were not identified in the results of C_{44} in Fig. 8(a). The shallow minima of C_{44} above 4 T up to 11 T correspond to the transition from the paramagnetic phase I to the AFQ phase II. In Fig. 8(b), we show magnetic field dependence of $\Delta C_{44}/C_{44}$ at various temperatures. The results of 2.2, 3.0, and 4.0 K show the III-II transition around 4 T, indicated by arrows. As shown in the inset of Fig. 8(b), a hysteresis effect has been observed which suggest the first order class of the III-II transition. As will be shown in the phase diagram of Fig. 11, phase IV changes to the phase I with increasing fields at 5.2 K.

The magnetic field dependence of $\Delta C_{44}/C_{44}$ up to 11 T with $H\|[001]$ in Fig. 8(b) revealed the field induced I-II transition. In order to examine the II-I phase transitions in higher fields with $H\|[001]$, we have pursued ultrasonic measurements of C_{11} using the hybrid magnet (GAMA) up to 30 T in Tsukuba Magnet Laboratory. We choose the longitudinal C_{11} mode because of its definite ultrasonic echo signal as compared to the relatively faint echo signal in transverse ultrasonic modes. Figure 9 represents the magnetic field dependence of $\Delta C_{11}/C_{11}$ at 1.5 K for $H\|[001]$ from 5 T to 30 T. A sharp minimum at 26.3 T has been found. The behaviors in AFQ phase transition of C_{11} are very similar to the ones of C_{66} for $H\|[100]$ or [110].

Figure 10 represents the temperature dependence of $\Delta C_{11}/C_{11}$ under fields of 15, 17, 18, 20, and 30 T. The C_{11} shows minima corresponding to the I-II phase transition, indicated by arrows, around 4 K and below 20 T. The minima shift slightly to lower temperatures with increasing fields. No anomaly in the result at 30 T indicates the absence of the I-II transition. The distinct difference between the results of 20 T and 30 T suggests that phase II closes in the vicinity of critical field $H_{C[001]}$=26.3 T.

Figure 11 represents the magnetic phase diagram in fields along the principal [001]-axis up to 30 T. The gray circles, solid squares, solid triangles, solid reversed triangles, and solid diamonds are the present results of C_{66} and C_{44}. The open triangles and open reversed triangles represent the transitions in the present results of C_{11} obtained by using the hybrid magnet. There are three ordered phases, the AFQ phase II, AFM phase III, and phase IV in addition to the paramagnetic phase I. In the phase III, subphase III$''_{001}$ exists between 2 T and 4 T. The magnetic neutron scattering in subphase III$''$ on HoB_2C_2 has not been reported yet. On the analogy of a similar subphase III$'$ on DyB_2C_2, the magnetic structure of subphase III$''_{001}$ for $H\|[110]$ on HoB_2C_2 is expected to be the altered form of AFM structure in phase III,

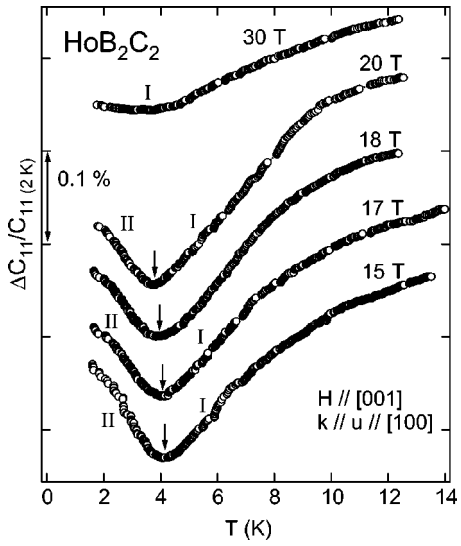

FIG. 10. Relative change of the elastic constant $\Delta C_{11}/C_{11}$ as a function of temperature at frequencies of 52 MHz under various field applied along the [001]-axis.

which the magnetic moments are partly rotated to the advantageous direction for the external magnetic field.[25] On the other hand, the boundary of phase III''_{001} for $H\|[001]$ has not been observed by magnetization measurement on HoB_2C_2.[8] Therefore, the origin of phase III''_{001} would be different from phase III''_{011}.

As one can see in the inset of Fig. 11, the four phases meet each other at the tetracritical point $T^* \sim 4.5$ K and $H^* \sim 3.0$ T. It is notable that the I-II and IV-III phase boundaries approach the tetracritical point tangential to each other,

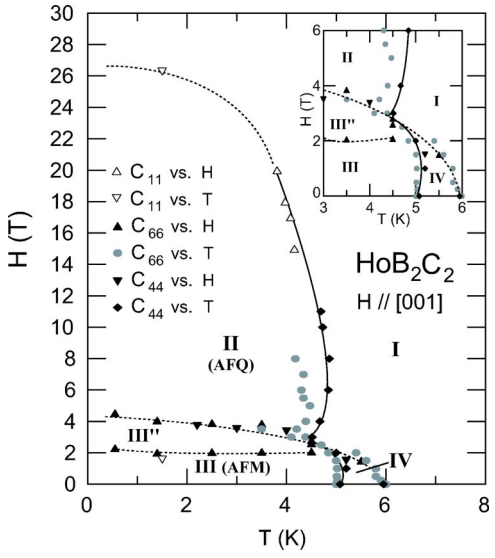

FIG. 11. Magnetic *H-T* phase diagrams of HoB_2C_2 with fields applied along the [001]-axis. Data points were determined from the elastic anomalies in C_{66} vs T (grey circles), C_{66} vs H (solid triangles), C_{44} vs H (solid reverse triangles), C_{44} vs T (solid diamonds), C_{11} vs T (open reverse triangles), and C_{11} vs H (open triangles) as shown in Figs. 7–9. Inset shows expanded view of tetracritical point. Solid and dotted lines are guides for the eyes.

due to the interplay of several order parameters. Similar multicritical phenomena appear on the *H-T* phase diagram of anisotropic AFM systems.[36,37] The hysteresis effect across the II-III phase boundary ensures the first order transition, and the discontinuity of the elastic constants at the IV-III transition points may also indicate the first order transition.

The vertical I-II phase boundary from 4 T to 20 T is determined by the minima in temperature dependence of C_{44} and C_{11}. There is a difference between the data-plots C_{66} and C_{44} that may be due to the mode difference or sample setting. We use the data of C_{44} to obtain the I-II transition in high field. The point at 26.3 T obtained by C_{11} in Fig. 9 suggests an upper phase boundary of the AFQ phase II in fields. The closed magnetic diagram of the AFQ phase in the present HoB_2C_2 resembles the closed behavior in the AFQ phase II in $Ce_{0.5}La_{0.5}B_6$.[38]

IV. CONCLUDING REMARKS

We have measured the elastic constants C_{11}, $(C_{11}-C_{12})/2$, C_{44}, and C_{66} of HoB_2C_2. The softening of these modes is due to the pseudotriplet ground state of the system. The minima or kinks of C_{11}, C_{44}, and C_{66} were useful in particular to determine the transition points in fields. We have obtained the *H-T* phase diagrams of HoB_2C_2 for the fields along the principal [001]-axis and in the basal *x-y* plane. In the *H-T* phase diagrams, there exists a tetracritical point at $T^* \sim 5.5$ K, $H^* \sim 0.75$ T for the basal plane and $T^* \sim 4.5$ K, $H^* \sim 3.0$ T for the principal [001]-axis, where two different interactions, magnetic dipole, and electric quadrupole, are competing with each other.

The AFQ phase II is stable even in fields of $H_{C[001]}=26.3$ T along the [001] axis at absolute zero, while the phase boundary shrinks to be $H_{C[110]}=3.8$ T for fields along the [110]-axis and $H_{C[100]}=2.0$ T for [100]-axis. This anisotropy in the critical fields $H_{C[001]} \gg H_{C[110]} > H_{C[100]}$ in HoB_2C_2 is dominated by the anisotropy of the RKKY-type quadrupole intersite interaction mediated by the conduction electrons in the tetragonal system. The de Haas-van Alphen measurements by Watanuki *et al.* revealed the main Fermi surface to have a columnar shape indicating two-dimensional character of the system.[39] The band calculation of LaB_2C_2 also shows the two-dimensional properties, reflecting the strong hybridization of the 5*d* orbitals of La with the 2*p* orbitals in B-C sheets.[40] The anisotropic band structure will play a role in the anisotropic quadrupole intersite interaction, which brings about the anisotropic behavior of the AFQ phase of HoB_2C_2 and DyB_2C_2 under magnetic fields.

It is useful to demonstrate the symmetry properties of the quadrupole moments under the applied fields along the high symmetry [100]-, [110]-, and [001]-axis. One may apply the symmetry argument of AFQ order parameters in cubic CeB_6, which was proposed by Shiina *et al.*,[41–43] to the present tetragonal HoB_2C_2 system. For a finite magnetic field, the symmetry of the system is lowered to keep the field induced dipole moment, namely angular momentum J_x, J_y, and J_z to be invariant. In the case of CeB_6, due to the Γ_5-type AFQ order parameter, linear combinations of quadrupole moments

result in cubic symmetry. In an applied magnetic field, the highest symmetry axis for these moments are related to field directions as follows: O_{xy} for $H\|[001]$, $O_{yz}+O_{zx}$ for $H\|[110]$, and $O_{yz}+O_{zx}+O_{xy}$ for $H\|[111]$ in cubic symmetry O_h.

In the case of tetragonal HoB_2C_2, when a field is applied along the [001]-axis, the local symmetry of the rare earth ion of C_{4h} is lowered to C_4 symmetry, while fields applied [100]- or [110]-axes change C_{4h} to C_2. Since the [001]-axis of Γ_2-type quadrupole O_{xy} and/or O_2^2 has a highest symmetry of three principal [100]-, [110]-, and [001]-axis, this causes no modulation in the Γ_2-type quadrupole when $H\|[001]$. As a consequence, the Γ_2-type AFQ order parameter O_{xy} and/or O_2^2 would be stuck on the basal plane even in magnetic field parallel to the basal plane due to the tetragonality of the system.

ACKNOWLEDGMENTS

The authors would like to thank J. Igarashi, O. Sakai, R. Shiina, and H. Onodera for fruitful discussions. The present work was supported by a Grant-in-Aid for Scientific Research Priority Area "Skutterudite" (No. 15072206) of the Ministry of Education, Culture, Sports, Science and Technology. One of the authors (T. Y.) was supported by Research Fellowships of the Japan Society for the Promotion of Science for Young Scientists in the present research.

*Also at Institute of Pure and Applied Physical Sciences, University of California at San Diego, La Jolla, California 92093, USA.

[1] K. Segawa, A. Tomita, K. Iwashita, M. Kasaya, T. Suzuki, and S. Kunii, J. Magn. Magn. Mater. **104–107**, 1233 (1992).

[2] S. Nakamura, T. Goto, S. Kunii, K. Iwashita, and A. Tamaki, J. Phys. Soc. Jpn. **63**, 623 (1994).

[3] T. Goto, Y. Nemoto, Y. Nakano, S. Nakamura, T. Kajitani, and S. Kunii, Physica B **281&282**, 586 (2000).

[4] J. M. Effantin, J. Rossat-Mignod, P. Burlet, H. Bartholin, S. Kunii, and T. Kasuya, J. Magn. Magn. Mater. **47&48**, 145 (1985).

[5] O. Sakai, R. Shiina, H. Shiba, and P. Thalmeier, J. Phys. Soc. Jpn. **66**, 3005 (1997).

[6] P. Link, A. Gukasov, J. M. Mignot, T. Matsumura, and T. Suzuki, Phys. Rev. Lett. **80**, 4779 (1998).

[7] H. Yamauchi, H. Onodera, K. Ohoyama, T. Onimaru, M. Kosaka, M. Ohashi, and Y. Yamaguchi, J. Phys. Soc. Jpn. **68**, 2057 (1999).

[8] H. Onodera, H. Yamauchi, and Y. Yamaguchi, J. Phys. Soc. Jpn. **68**, 2526 (1999).

[9] K. Kaneko, H. Onodera, H. Yamauchi, K. Ohoyama, A. Tobo, and Y. Yamaguchi, J. Phys. Soc. Jpn. **69**, 3762 (2000).

[10] K. Ohoyama, K. Kaneko, K. Indoh, H. Yamauchi, A. Tobo, H. Onodera, and Y. Yamaguchi, J. Phys. Soc. Jpn. **70**, 3291 (2001).

[11] J. van Duijn, J. P. Attfield, and K. Suzuki, Phys. Rev. B **62**, 6410 (2000).

[12] H. Yamauchi, H. Onodera, M. Ohashi, K. Ohoyama, T. Onimaru, M. Kosaka, M. Ohashi, and Y. Yamaguchi, J. Phys. Chem. Solids **60**, 1217 (1999).

[13] H. Yamauchi, K. Ohoyama, M. Sato, S. Katano, H. Onodera, and Y. Yamaguchi, J. Phys. Soc. Jpn. **71**, 94 (2002).

[14] Y. Tanaka, T. Imai, T. Nakamura, H. Yamauchi, H. Onodera, K. Ohoyama, and Y. Yamaguchi, J. Phys.: Condens. Matter **11**, L505 (1999).

[15] Y. Tanaka, T. Inami, S. W. Lovesey, K. S. Knight, F. Yakhou, D. Mannix, J. Kokubun, M. Kanazawa, K. Ishida, S. Nanao, T. Nakamura, H. Yamauchi, H. Onodera, K. Ohoyama, and Y. Yamaguchi, Phys. Rev. B **69**, 024417 (2004).

[16] J. Igarashi and T. Nagao, J. Phys. Soc. Jpn. **72**, 1279 (2003).

[17] S. W. Lovesey and K. S. Knight, Phys. Rev. B **64**, 094401 (2001).

[18] K. Hirota, N. Oumi, T. Matsumura, H. Nakao, Y. Wakabayashi, Y. Murakami, and Y. Endoh, Phys. Rev. Lett. **84**, 2706 (2000).

[19] T. Matsumura, N. Oumi, K. Hirota, H. Nakao, Y. Murakami, Y. Wakabayashi, T. Arima, S. Ishihara, and Y. Endoh, Phys. Rev. B **65**, 094420 (2002).

[20] T. Matsumura, N. Oumi, K. Hirota, H. Nakao, Y. Wakabayashi, and Y. Murakami, J. Phys. Soc. Jpn. **71**, 91 (2002).

[21] K. Ohoyama, H. Yamauchi, A. Tobo, H. Onodera, H. Kadowaki, and Y. Yamaguchi, J. Phys. Soc. Jpn. **69**, 3401 (2000).

[22] A. Tobo, T. Ohmori, T. Matsumura, K. Hirota, N. Oumi, H. Yamauchi, K. Ohoyama, H. Onodera, and Y. Yamaguchi, Physica B **312&313**, 853 (2002).

[23] K. Kaneko, K. Ohoyama, S. Katano, M. Matsuda, H. Onodera, and Y. Yamaguchi, J. Phys. Soc. Jpn. **71**, 3024 (2002).

[24] K. Ohoyama, K. Indoh, A. Tobo, H. Onodera, and Y. Yamaguchi, J. Phys. Soc. Jpn. **71**, 1746 (2002).

[25] K. Indoh, A. Tobo, H. Yamauchi, K. Ohoyama, and H. Onodera, J. Phys. Soc. Jpn. **73**, 669 (2004).

[26] O. Zaharko, W. Sikora, F. Bialas, U. Staub, and T. Nakamura, Phys. Rev. B **69**, 224417 (2004).

[27] H. Shimada, H. Onodera, H. Yamauchi, A. Tobo, K. Ohoyama, and Y. Yamaguchi, J. Phys. Soc. Jpn. **70**, 1705 (2001).

[28] P. Thalmeier and B. Luthi, in *Handbook on the Physics and Chemistry of Rare Earths*, edited by K. A. Gschneider, Jr. and L. Eyring (North-Holland, Amsterdam, 1991), Vol. 14, p. 311.

[29] T. Yanagisawa, T. Goto, Y. Nemoto, S. Miyata, R. Watanuki, and K. Suzuki, Phys. Rev. B **67**, 115129 (2003).

[30] H. Yamauchi, H. Onodera, K. Kaneko, A. Tobo, K. Ohoyama, and Y. Yamaguchi, J. Magn. Magn. Mater. **226–230**, 1134 (2001).

[31] M. Hiroi, S. Kobayashi, M. Sera, N. Kobayashi, and S. Kunii, J. Phys. Soc. Jpn. **66**, 1762 (1997).

[32] T. Tayama, T. Sakakibara, K. Tenya, H. Amitsuka, and S. Kunii, J. Phys. Soc. Jpn. **66**, 2268 (1997).

[33] O. Suzuki, T. Goto, S. Nakamura, T. Matsumura, and S. Kunii, J. Phys. Soc. Jpn. **67**, 4243 (1998).

[34] M. Akatsu, T. Goto, Y. Nemoto, O. Suzuki, S. Nakamura, and S. Kunii, J. Phys. Soc. Jpn. **71**, 205 (2002).

[35] K. Kubo and Y. Kuramoto, J. Phys. Soc. Jpn. **72**, 1859 (2003).

[36] H. Rohrer and Ch. Gerber, Phys. Rev. Lett. **38**, 909 (1977).

[37] A. D. Bruice and A. Aharony, Phys. Rev. B **11**, 478 (1975).

[38] M. Akatsu, T. Goto, O. Suzuki, Y. Nemoto, S. Nakamura, S.

Kunii, and G. Kido, Phys. Rev. Lett. **93**, 156409 (2004).
[39] R. Watanuki, T. Terashima, and K. Suzuki, J. Phys. Soc. Jpn. **71**, 693 (2002).
[40] H. Harima, New properties of matter due to ordering and fluctuation orbitals Newsletter of Scientific Research on Priority Area (B), 2000, Vol. 2, No. 2, p. 24.
[41] R. Shiina, H. Shiba, and P. Thalmeier, J. Phys. Soc. Jpn. **66**, 1741 (1997).
[42] R. Shiina, O. Sakai, H. Shiba, and P. Thalmeier, J. Phys. Soc. Jpn. **67**, 941 (1998).
[43] O. Sakai, R. Shiina, and H. Shiba, J. Phys. Soc. Jpn. **72**, 1534 (2003).